IOP Conf. Series: Journal of Physics: Conf. Series **828** (2017) 012002 doi:10.1088/1742-6596/828/1/012002

# Effects of magnetic field and hydrostatic pressure on the distorted triangular lattice antiferromagnet $RbFeBr_3$

**Nobuyuki Kurita, Hidekazu Tanaka**

Department of Physics, Tokyo Institute of Technology, Meguro-ku, Tokyo 152-8551, Japan

E-mail: kurita@phys.titech.ac.jp

**Abstract.** We report on magnetization measurements of $RbFeBr_3$ single crystals. At ambient pressure, the field–temperature phase diagram has been determined up to 70 kOe for $H \parallel c$. It is found that the application of magnetic field for $H \parallel c$ expands the low temperature phase with the triangular spin structure ($T < T_{N2}$) and suppresses the partially disordered phase ($T_{N2} < T < T_{N1}$). When hydrostatic pressure is applied under 100 Oe for $H \parallel c$, the magnetization anomaly related to $T_{N1}$ shifts to lower temperatures and is no more detectable at $P \geq 1.0$ GPa.

## 1. Introduction

Over the past decades, hexagonal $ABX_3$-type compounds has continued to attract considerable interest as a model system of triangular-lattice antiferromagnets (TLA). The spin chains consisting of magnetic $B^{2+}$ ions centered at $BX_6$ octahedra align along the $c$-axis and form triangular lattices in the $c$-plane. Since the exchange coupling between the spin chains are antiferromagnetic (AF), a rich variety of quantum phenomena have been observed owing to the geometric spin frustration characteristic of TLA [1].

As is the case with typical $ABX_3$ series, $RbFeBr_3$ crystallizes in the hexagonal $CsNiCl_3$ structure with the space group $P6_3/mmc$ at room temperature. With decreasing temperature, this compound undergoes successive structural phase transitions at 109 K and 39.5 K to a lower symmetry phase which is found to be ferroelectric along the $c$-axis [2, 3, 4]. The crystal structure of the low temperature phase is of the hexagonal $KNiCl_3$-type with $P6_3cm$ where the triangular lattices are distorted. Accordingly, there exist two kinds of interlayer exchange interactions so that the spin frustration is partially released in the $c$-plane. Several experiments have revealed that two AF phase transitions occur at $T_{N1} = 5.6$ K and $T_{N2} = 2.0$ K in the ferroelectric phase [5, 6, 7]. The successive phase transition in the XY-type disordered triangular antiferromagnets is consistent with theoretical results [8, 9]. Recent neutron diffraction measurements in the absence of applied field have shown that the spin configuration is partially disordered (PD) in the intermediate phase ($T_{N2} < T < T_{N1}$) and triangular with spin directions slightly tilt from 120° to each other at lower temperatures below $T_{N2}$ [7]. In the PD phase, one of three spin chains is uncorrelated and the other two spin chains couple antiferromagnetically.

It is known that magnetic $Fe^{2+}$ ions in an octahedral environment can be described by effective spin $S = 1$ at low temperatures well below $\lambda/k_B \simeq 150$ K where $\lambda$ is the spin-orbit coupling [10]. Because the $FeBr_6$ octahedrons are trigonally elongated, $RbFeBr_3$ has the singlet

ground state and the doublet first excited state which are separated by the large easy-plane single-ion anisotropy $D(S^z)^2$ [11, 12]. In $RbFeBr_3$, exchange interactions are predominant over the magnetic anisotropy so that three dimensional magnetic orders occur in the absence of magnetic field.

In this proceedings, we investigate the field and pressure effects on the magnetic phase transitions of $RbFeBr_3$, via magnetization measurements using single crystals.

## 2. Experimental Details

Single crystals of $RbFeBr_3$ were grown via the vertical Bridgman method from a stoichiometric mixture of constituent elements sealed in an evacuated quartz tube. The ingredients were dehydrated in vacuum by heating up to 150°C for three days. The temperature at the center of the furnace was set at 660°C and the crystals were lowered at a rate of 3 mm/hour. We repeated the same procedure after the removal of impurities and imperfect crystals.

The magnetization measurements were carried out down to 1.8 K under magnetic fields of up to 70 kOe using a SQUID magnetometer (MPMS-XL, Quantum Design). High pressure magnetization was measured up to a pressure of 1.2 GPa using a clamped piston cylinder pressure device. Daphne 7373 (Idemitsu Kosan), which remains in the liquid state up to $\sim$ 2 GPa at room temperature [13], was used as a pressure-transmitting medium. The pressure generated in the sample space was calibrated at a low temperature by the change in the superconducting transition temperature $T_c$ of tin under $H = 10$ Oe. The high-pressure magnetization data are corrected for the background contributions.

## 3. Results and Discussions

Figure 1(a) shows temperature dependence of magnetic susceptibility $\chi\,(=M/H)$ of $RbFeBr_3$ under 1 kOe for $H \parallel c$ and $H \perp c$. The obtained $\chi(T)$ data are in good agreement with previous results [11]. $\chi(T)$ for $H \parallel c$ exhibits a broad peak around 15 K followed by a rapid decrease with decreasing temperature, while $\chi(T)$ for $H \perp c$ shows a continuous increase down to the lower temperatures. The anisotropic behaviors in $\chi(T)$ with respect to the field direction are mostly attributable to the large easy-plane single-ion anisotropy $D(S^z)^2$ due to the trigonal crystalline field [14]. Figure 1(b) shows the low temperature $\chi(T)$ data of $RbFeBr_3$ under 1 kOe. Arrows denote AF transition temperatures $T_{N1} = 5.6$ K and $T_{N2} = 2.0$ K reported by the previous specific heat study in zero field [5]. For $H \parallel c$, one can see two slight anomalies both at $T_{N1}$ and $T_{N2}$. For $H \perp c$, $\chi(T)$ exhibits a clear jump at $T_{N1}$ while no sign associated with $T_{N2}$ was identified.

Below, we focus on results obtained for $H \parallel c$. Figure 2 shows the $\chi(T)$ and $d\chi/dT(T)$ data of $RbFeBr_3$ under several fields up to 70 kOe for $H \parallel c$. As indicated by arrows in the $d\chi/dT(T)$ data under 10 kOe, we assign $T_{N1}$ and $T_{N2}$ as temperatures where $d\chi/dT(T)$ shows a sudden decrease with decreasing temperature. With increasing field, no significant change is found for $T_{N1}$ while the magnetization anomaly related to $T_{N2}$ shifts to higher temperatures and evolves to a cusplike peak. It is noted that the similar cusplike peaks in $\chi(T)$ are observed at the AF transition temperatures for the field-induced ordered phase of the related compounds $CsFeCl_3$ [15] and $CsFeBr_3$ [16]. Contrary to the case with $RbFeBr_3$, these compounds have the gapped singlet ground state in zero field since exchange interactions are not strong enough to produce the long range order [18, 19, 20]. When magnetic field is applied above the critical values $H_c \sim 40$ kOe for $CsFeCl_3$ [15, 17] and $\sim 30$ kOe for $CsFeBr_3$ [16], these compounds exhibit field-induced AF phase transitions. Figure 3 illustrates the magnetic phase diagram of $RbFeBr_3$ up to 70 kOe for $H \parallel c$, determined via the present magnetization measurements. It is found that application of magnetic field for $H \parallel c$ on this compound stabilizes the triangular spin phase (phase II) and suppresses the PD phase (phase I) whereas there is little effect on $T_{N1}$.

Next, we present results of the high-pressure magnetization measurement performed under low magnetic field. Figure 4 shows $\chi(T)$ data of $RbFeBr_3$ at several pressures up to 1.2 GPa

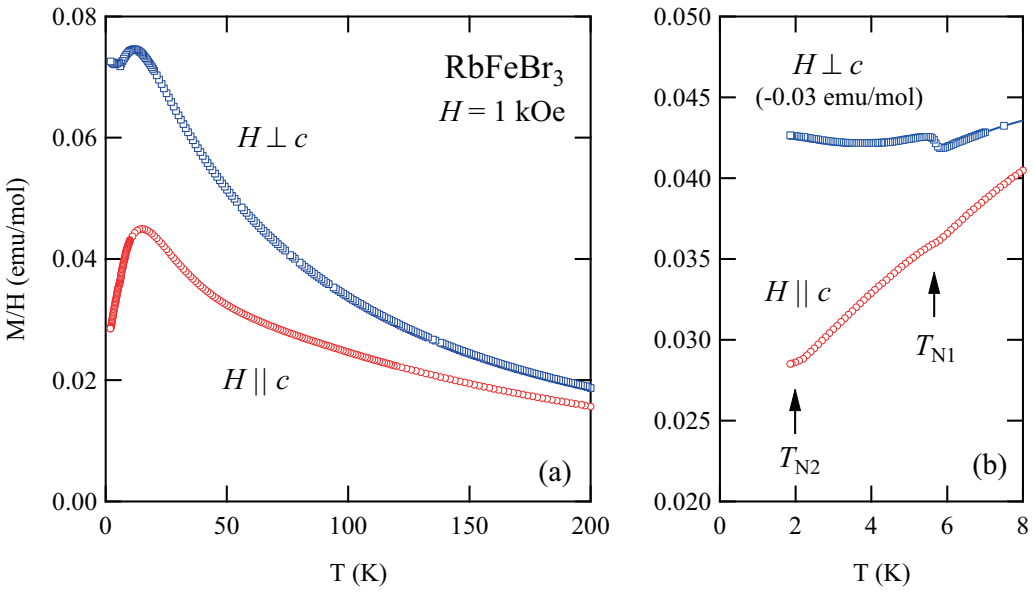


**Figure 1.** (Color online) (a) Magnetic susceptibility $\chi$ ($=M/H$) vs $T$ of $RbFeBr_3$ under 1 kOe for $H \parallel c$ and $H \perp c$. (b) Expanded view of $\chi(T)$ data at low temperatures. $\chi(T)$ for $H \perp c$ is shifted in the longitudinal direction by $-0.03$ emu/mol. Arrows denote $T_{N1}$ and $T_{N2}$ reported by the previous specific heat study [5].

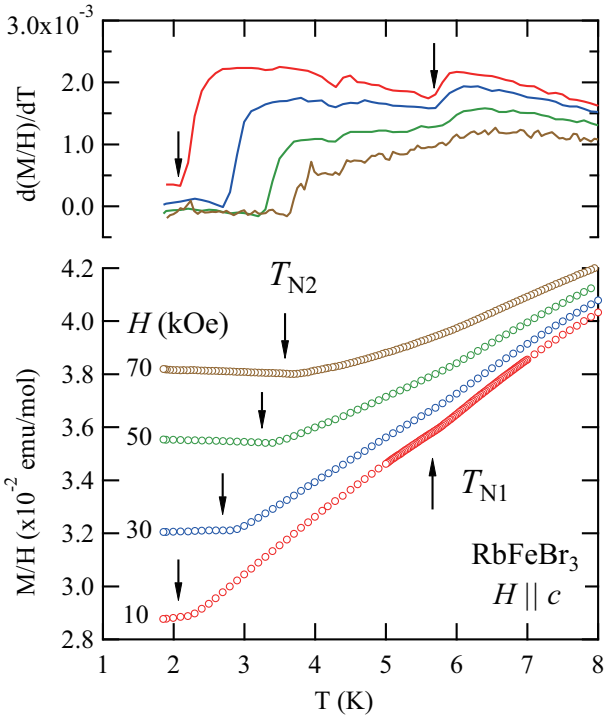


**Figure 2.** (Color online) (a) Temperature dependence of $\chi$ ($=M/H$) and $d\chi/dT$ of $RbFeBr_3$ for $H \parallel c$ under several fields up to 70 kOe. Arrows indicate $T_{N1}$ and $T_{N2}$ deduced from anomalies in $d\chi/dT(T)$ data.

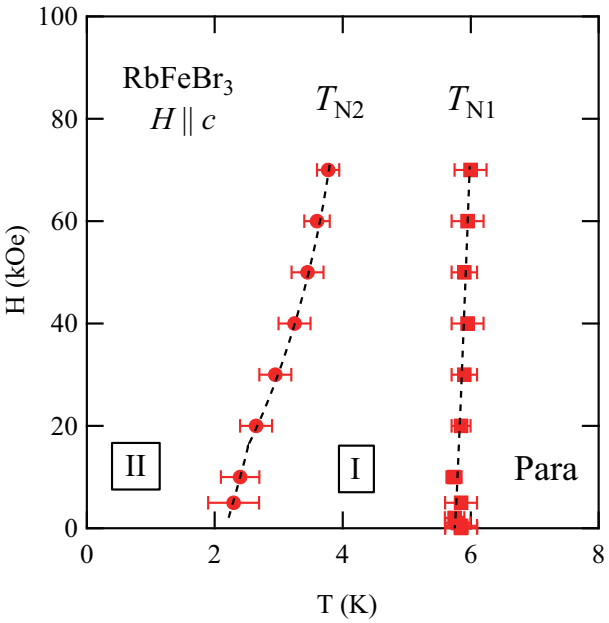


**Figure 3.** (Color online) Field-temperature phase diagram of $RbFeBr_3$ for $H \parallel c$ obtained from the magnetization measurements. Dashed curves are guides to the eyes. Spin configurations in the phases I and II are partially disordered and triangular structures, respectively [5].

under 100 Oe for $H \parallel c$. For clarity, the data are shifted arbitrarily in the longitudinal direction. The lowest measured temperature at high-pressures is limited to 2 – 3 K because of the Meissner effect induced by a superconducting transition of tin, which is included in the sample space as a pressure sensor. At ambient pressure, as compared to results under 1 kOe shown in Fig. 1(b), $\chi(T)$ under 100 Oe exhibits a clear jump at $T_{N1}$ while there is no obvious signature of $T_{N2}$. With increasing pressure, the magnetization anomaly due to $T_{N1}$ shifts to lower temperatures and is no more detectable at $P \geq 1.0$ GPa.

Here, the role of hydrostatic pressure on $RbFeBr_3$ is discussed. Since the intrachain exchange interaction $J_0$ is an order of magnitude larger than the interchain exchange interactions [11, 12], we only consider pressure evolution of $J_0$. In this compound, there exist both AF and ferromagnetic (FM) paths of exchange interactions. Considering the fact that $J_0$ is AF, the AF exchange interaction dominates over the ferromagnetic (FM) exchange interaction. Thus, the primary effect of pressure could be to enhance the FM intrachain exchange interaction since $T_{N1}$ is suppressed by applying hydrostatic pressure. This scenario is consistent with high pressure studies of $CsFeBr_3$ [21] and $CsFeCl_3$ [15]. In $CsFeBr_3$ where $J_0$ is AF, application of hydrostatic pressure decreases the AF transition temperature for the field-induced ordered phase and increases the transition field $H_c$. In $CsFeCl_3$ where $J_0$ is FM, in contrast, the field-induced ordered phase moves toward a higher-temperature and lower-field with increasing hydrostatic pressure, and, eventually, a pressure-induced magnetic phase transition occurs at the critical pressure of 0.9 GPa.

## 4. Conclusions

To conclude, we have performed magnetization measurements of $RbFeBr_3$ single crystals under fields up to 70 kOe at ambient pressure and under 100 Oe at high pressures up to 1.2 GPa. At ambient pressure, the obtained field–temperature phase diagram for $H \parallel c$ indicates that, with increasing magnetic field, the triangular ground state and PD phase become stabilized and

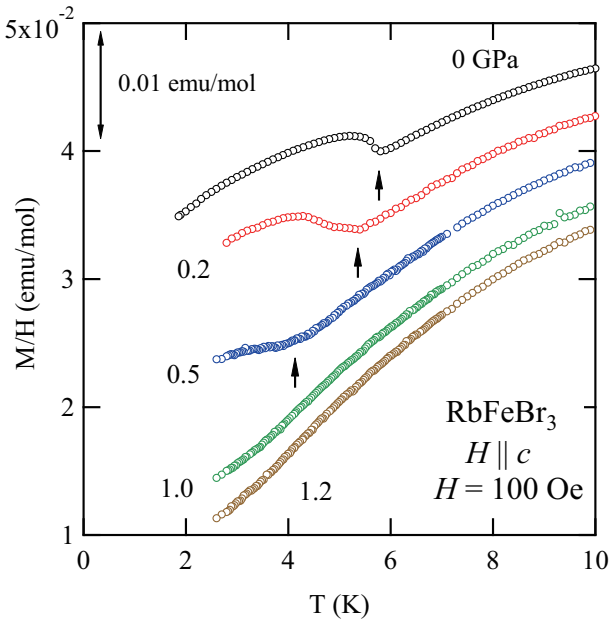


**Figure 4.** (Color online) $M/H$ vs $T$ of $RbFeBr_3$ under 100 Oe for $H \parallel c$ at pressures up to 1.2 GPa. Arrows indicate $T_{N1}$. For clarity, the data are shifted arbitrarily in the longitudinal direction.

suppressed, respectively. With increasing pressure under 100 Oe, $T_{N1}$ decreases and no sign of $T_{N1}$ is detectable at $P \geq 1.0$ GPa. This suggests that the primary role of hydrostatic pressure on this compound could be to enhance the FM intrachain exchange interactions.

## Acknowledgments

This work was supported by Grants-in-Aid for Scientific Research (A) Nos. 23244072 and 26247058, (C) No. 16K05414 from Japan Society for the Promotion of Science.

## References

[1] Collins M F and Petrenko O A 1997 *Can. J. Phys.* **75**, 605
[2] Eibschütz M, Davidson G R and Cox D. E 1973 *AIP Conf. Proc.* **18**, 386
[3] Harrison A and Visser D 1989 *J. Phys.: Condens. Matter.* **1** 733.
[4] Mitsui T, Machida K, Kato T and Iio K, 1994 *J. Phys. Soc. Jpn.* **63** 839
[5] Achiwa N 1969 *J. Phys. Soc. Jpn.* **27** 561
[6] Kato T, Nishino T, Morishita K, Tanaka H and Iio K 1998 *J. Mag. Mag. Mater.* **177-181** 831
[7] Nishiwaki Y, Oosawa A, Kakurai K, Kaneko K, Tokunaga M and Kato T 2011 *J. Phys. Soc. Jpn.* **80** 084711
[8] Kawamura H 1990 *J. Phys. Soc. Jpn.* **101** 545
[9] Plumer M L, Caillé A and Kawamura H 1991 *Phys. Rev. B* **44** 4461
[10] Inomata K and Oguchi T 1967 *J. Phys. Soc. Jpn.* **23** 771.
[11] Lines M E and Eibschütz M 1975 *Phys. Rev. B* **11** 4583
[12] Harrison A and Visser D 1989 *Phys. Lett.* **137A** 79.
[13] Murata K, Yoshino H, Yadav H O, Honda Y and Shirakawa N 1977 *Rev. Sci. Instrum.* **68**, 2490
[14] Adachi K, Takeda K, Matsubara F, Mekata M and Haseda T 1983 *J. Phys. Soc. Jpn.* **52** 2202
[15] Kurita N and Tanaka H 2016 *Phys. Rev. B* **94** 104409
[16] Tanaka Y, Tanaka H, Ono T, Oosawa A, Morishita K, Iio K, Kato T, Aruga-Katori H, Bartashevich M. I and Goto T 2001 *J. Phys. Soc. Jpn.* **70**, 3068; 2007 *J. Phys. Soc. Jpn.* **76**, 108001
[17] Haseda T, Wada N, Hata M and Amaya K 1981 *Physica B* **108** 841
[18] Yoshizawa H, Kozukue W and Hirakawa K., 1980 *J. Phys. Soc. Jpn.* **49** 144
[19] Bocquet S 1988 *Phys. Rev. B* **37** 7840

[20] Dorner B, Visser D, Steigenberger U, Kakurai K and Steiner M 1988 *Z. Phys. B* **72** 487
[21] Momosaki Y, Ono T, and Tanaka H unpublished data